IEEE Access
Multidisciplinary | Rapid Review | Open Access Journal

IEEE RELIABILITY SOCIETY SECTION

Received 1 February 2024, accepted 11 March 2024, date of publication 19 March 2024, date of current version 25 March 2024.

Digital Object Identifier 10.1109/ACCESS.2024.3377691

RESEARCH ARTICLE

Novel Adversarial Unsupervised Subdomain Adaption Multi-Channel Deep Convolutional Network for Cross-Operating Fault Diagnosis of Rolling Bearings

BO ZHANG[1], TIANLONG HUO[1,2], ZHENG LIU[1], BAOQUAN HU[2], HEYUE HUANG[1], ZEHAI REN[2,3], AND JIANBO JI[1]

[1]School of Electronic Information and Automation, Guilin University of Aerospace Technology, Guilin 541004, China
[2]School of Mechanical and Electrical Engineering, Lanzhou University of Technology, Lanzhou 730050, China
[3]School of Mechanical Engineering, Guilin University of Aerospace Technology, Guilin 541004, China

Corresponding author: Tianlong Huo (htl@guat.edu.cn)

This work was supported in part by the National Natural Science Foundation of China under Grant 62263009, in part by the Fundamental Ability Enhancement Project for Young and Middle-Aged University Teachers in Guangxi Province under Grant 2023KY0810, and in part by the Natural Science Foundation of Guilin University of Aerospace Technology under Grant XJ22KT25.

ABSTRACT Rolling bearings in production practice usually serve in a healthy state. Some fault state labels are scarce or even no labels, resulting in unbalanced data categories. Meanwhile, frequent working condition switching results in significant differences in data distribution among working conditions, and labeled data in some working states cannot be fully utilized. To deal with the challenge of low fault identification accuracy caused by these practical factors, this paper proposed a novel adversarial unsupervised subdomain adaption multi-channel deep convolutional network (ASMDCN). Firstly, a parallel three-channel depth feature extraction module is built, and a multi-scale convolution kernel is used to fully extract the rich features of vibration signals under various working conditions. Secondly, a novel loss function is designed to adequately consider the classification difficulty of samples and the degree of class imbalance. Finally, the adversarial training strategy is used to force the feature extractor to extract the domain invariant features, and the Local Maximum Mean discrepancy (LMMD) is used to align the global and related subdomains of the source and target domains. The experimental results show that the designed feature extraction can fully extract the domain-invariant features of the rolling bearings under different working conditions. Under the proposed objective function optimization, the network model can fully align the features of multi-source and single-target domain under unbalanced data and has strong generalization performance.

INDEX TERMS Intelligent cross-domain fault diagnosis, unbalanced data, adversarial domain adaptation, subdomain adaptation.

I. INTRODUCTION

As the core part of large-scale mechanical equipment, rotating machinery plays a considerable role in aerospace, communication and transportation, petrochemical, and other fields [1], [2], [3]. However, these sizeable mechanical equipment usually work in harsh environments, and rolling bearings, as their key components, are vulnerable to impact loads, mechanical fatigue, frequent switching of working conditions, improper maintenance, and other reasons for failure [4], [5], [6]. Once the failure occurs, it may cause substantial economic losses and negative social impact. Therefore, condition monitoring and fault diagnosis of rolling bearings can accurately assess potential risks and make predictive maintenance decisions, which is significant to mechanical equipment's safe and stable operation [7], [8].

The associate editor coordinating the review of this manuscript and approving it for publication was Zhaojun Steven Li.

In the past, the traditional methods based on vibration signal processing and feature extraction have achieved remarkable results [9], [10], [11]. However, this shallow model method is limited in the actual industry because it relies too much on expert system knowledge [12].

With the widespread application and rapid development of artificial intelligence technology in various industries, the deep learning fault diagnosis method has become a research hotspot due to its end-to-end structure and the ability to extract high-level feature representation of signals directly [13], [14], [15]. Typical methods are based on convolutional neural networks (CNN) [16], recurrent neural networks [17], autoencoders [18], and graph convolutional neural networks (GCNN) [19]. Among them, the method based on convolutional neural networks shows excellent diagnostic performance in fault diagnosis. XING et al. [20] directly send vibration signals to the proposed new 1D-CNN, which had high diagnostic accuracy for unbalanced data. Zhang et al. [21] applied 1D-CNN to construct a multi-scale residual attention network, which can learn multi-scale features of signals in a high-noise environment. Zhang et al. [22] designed an improved three-layer CNN structure to realize the fault diagnosis of bearing with multiple operating conditions. However, all the above studies are based on the assumption that the sample data is labeled and that the samples used for model training and the samples to be tested obey the same distribution. Due to production process constraints, rolling bearings need to switch working states frequently. Specific differences in data distribution exist, and data labels cannot be obtained under specific working conditions. If the above method is used directly, the diagnostic accuracy will decrease or fail.

Unsupervised domain adaption can effectively align the distribution difference between the source and target domain and diagnose the fault types of the target domain without labels. Li et al. [23] proposed a domain adversarial network framework based on correlation alignment (CORAL) with high diagnostic accuracy and good generalization for cross-domain diagnosis. Zhang et al. [24] proposed a domain additional network with a multi-scale attention mechanism, which used maximum mean discrepancy (MMD) to minimize the distribution difference between the source and target domains, achieving better diagnostic results for rolling bearings. Ferracuti et al. [25] used Wasserstein Distance (WD) as the distance measurement function of source and target domains, effectively diagnosing various faults and complex working conditions. Wan et al. [26] used Multiple Kernel MMD (MK-MMD) and a multi-domain discriminator to align the source and target domain data distribution. They achieved excellent migration effect in cross-operating fault diagnosis of bearings. The above research work has made outstanding achievements in the cross-operating unsupervised fault diagnosis of rolling bearings. However, the above methods mainly learn the global distribution difference between the source and target domains. If the subdomain data can be further considered and fine-grained information can be captured, the diagnosis results may be significantly improved.

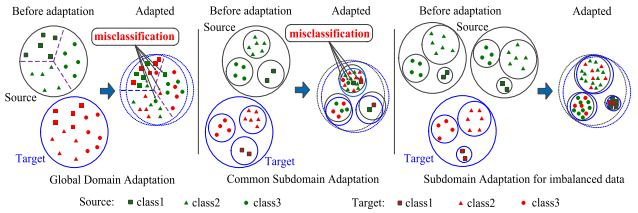

FIGURE 1. Problem description of the domain adaptation.

Aiming to capture fine-grained information, Zhu et al. [27] proposed a deep subdomain adaption network, which used LMMD to align the related subdomains of the two data domains. They achieved remarkable results in image migration recognition. In the field of bearing fault diagnosis, Liu et al. [28] proposed a deep adversarial subdomain adaption network, which used the simultaneous constraints of domain discriminator and LMMD to extract domain invariant and fine-grained features. Zhang et al. [29] proposed a hybrid adversarial data analysis network, which uses LMMD to realize subdomain adaption and has robust diagnostic performance in multiple transfer diagnosis. Xiao et al. [30] proposed a subdomain adaption deep transfer learning network for intelligent damage diagnosis of bridges. MK-LMMD was used to realize global and local alignment of the features of the two domains. Kavianpour et al. [31] proposed a class alignment network based on GCNN and adopted MK-LMMD to realize the alignment of subclass features. The above research work has made an outstanding contribution to cross-domain unsupervised subdomain adaption. However, the above studies are based on the assumption of the balanced distribution of data categories in two domains and utilize the single-source domain to train the model. In actual production, bearings are primarily operated under normal conditions. In other words, the normal sample size is large, and the fault sample is accidental, resulting in an imbalance in the fault category. In addition, bearings need to be switched frequently in various working conditions to complete a specific production process, and in some working conditions, we cannot obtain data and labels. Therefore, how to make full use of the unbalanced data with labels in multi-working states to diagnose unlabeled test samples is an urgent problem in the field of fault diagnosis.

Aiming at the above problems, this paper proposes an ASMDCN to fill the gap. As shown in Fig. 1, the left section uses global data alignment but does not consider subdomain data. Although the middle part considers the alignment of subdomain data, it ignores the influence of unbalanced data, eventually leading to misclassification. On the far right is our proposed method. The network framework employs unbalanced data under various working conditions to train the network and realizes high-precision unsupervised fault diagnosis of cross-operating rolling bearings. The contributions of this paper are as follows:

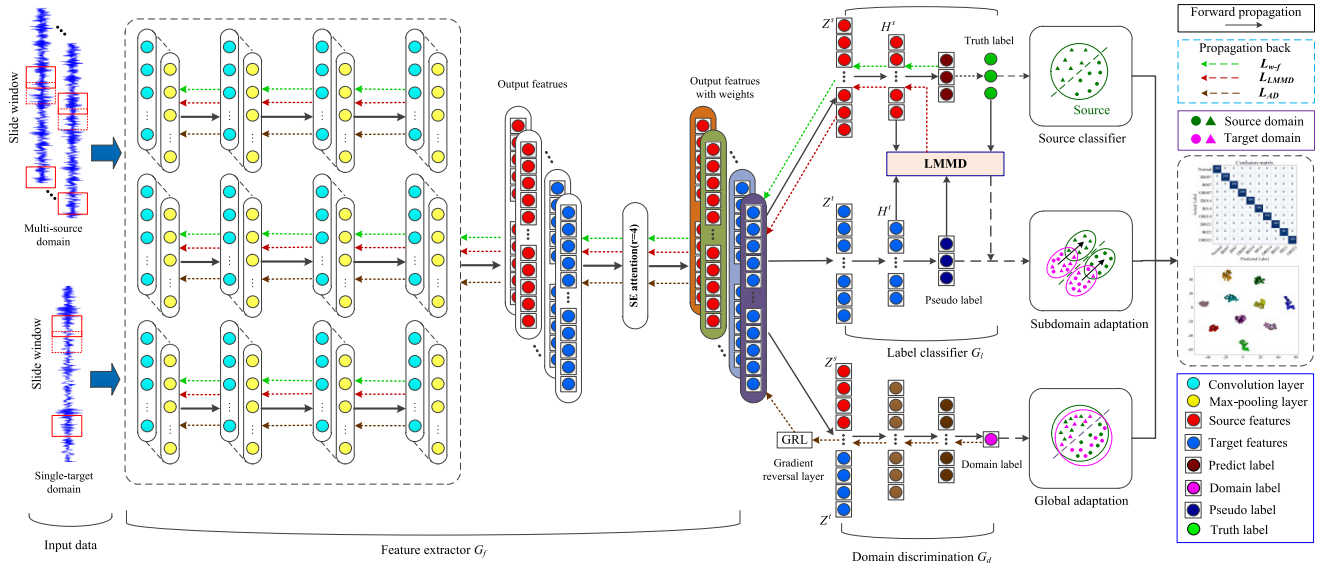

FIGURE 2. The proposed framework.

1) Considering the degree of unbalance of class data and the difficulty of sample classification, a new label loss function is proposed as a part of the overall objective function, achieving high-precision classification of class data unbalance.

2) The adaptive constraints of the adversarial domain are employed to guide the three-branch deep convolutional network to extract the domain-invariant features fully conducive to model classification. Simultaneously, LMMD is further used to align the related subdomains of the domains.

3) To enhance the model's generalization ability, the labeled source domains data under multiple working conditions and single working conditions unlabeled target domain data are used to train the model.

The rest of this paper is organized as follows: The second section introduces the problem definition and the basic theory of MMD. The third section presents the structure of the ASMDCN framework in detail. The fourth section introduces the experimental data used and the detailed experimental results. The fifth section gives the conclusion of this paper.

II. BASIC THEORY

A. PROBLEM DEFINITION

This paper mainly studies the cross-operating unsupervised intelligent fault diagnosis method of rolling bearings. Due to the limitations of the production process, rolling bearings usually need to be switched frequently under various working conditions. Therefore, we construct the multi-source domains $D_{s1} = \left\{\left(x_i^{s1}, y_i^{s1}\right)\right\}_{i=1}^{n_{s1}}, \cdots, D_{sn} = \left\{\left(x_i^{sn}, y_i^{sn}\right)\right\}_{i=1}^{n_{sn}} (n_s = n_{s1} + \cdots + n_{sn})$ with n_s labeled samples and target domain $D_t = \left\{\left(x_j^t\right)\right\}_{j=1}^{n_t}$ with n_t unlabeled samples, where x_i^{sn} is the i-th sample of n-th working conditions in the source domain, y_i^{sn} the corresponding label, x_j^t is the j-th sample in the target domain. We assume that multi-source domains $D_s = \{D_{s1}, \cdots, D_{sn}\}$ and target domain D_t have the same sample space $Y = \{1, 2, \cdots, N_C\}$, N_C represents the number of rolling bearing health status categories. Since both D_s and D_t are collected under different working conditions, their probability distributions are also different. Therefore, suppose $P = \{p_1, \cdots, p_n\}$ and q represent marginal probability distributions for D_s and D_t, respectively. In this paper, we employ labeled multi-source domains and unlabeled single-target domain to train the model to diagnose the health category of the target domain.

B. MMD

MMD is one of the most commonly used discrepancy measures approach in domain adaptation. The method maps two distributed data into a Hilbert space and calculates the difference. MMD is to find the continuous function $\phi : x \to R$ in the sample space and then calculate the mean of the samples of the two distributions on ϕ. The size of the difference reflects the degree of similarity of the different distributions. Let $X_s = \left\{x_i^s\right\}_{i=1}^{n_s}$ and $X_t = \left\{x_j^t\right\}_{j=1}^{n_t}$ obey the probability distributions p and q respectively, then the formula for MMD between the two datasets is as follows:

$$d_H(p, q) \triangleq \left\| E_p\left[\phi(X_s)\right] - E_q\left[\phi(X_t)\right] \right\|_H^2 \tag{1}$$

where H is reproducing kernel Hilbert space (RKHS). $\phi(\cdot)$ is a function that maps data to a Hilbert space. The above formula is called the overall probability measure in statistics. To further calculate the difference, the biased estimate of MMD can be used to replace it. The calculation formula is

TABLE 1. The structure and detailed parameters of the proposed ASMDCN.

Component	Layers		Detailed parameters	Output size	#Parameters
Feature extractor	Channel 1	Conv 1-1 / BN / ReL	out_channels=16, kernel_size=41, stride=2	16×492	672
		Max Pooling	kernel_size =3, stride =1	16×490	/
		Conv 1-2/ BN / ReL	out_ channels =32, kernel_size =21, stride =2	32×235	10784
		Max Pooling	kernel_size =3, stride =1	32×233	/
		Conv 1-3/ BN / ReL	out_ channels =64, kernel_size =11, stride =2	64×112	22592
		Max Pooling	kernel_size =3, stride =1	64×110	/
		Conv 1-4/ BN / ReL	out_ channels =128, kernel_size =9, stride =2	128×51	73856
		Max Pooling	kernel_size =3, stride =1	128×49	/
	Channel 2	Conv 2-1/ BN / ReL	out_ channels =16, kernel_size =7, stride =2	16×509	128
		Max Pooling	kernel_size =3, stride =1	16×507	/
		Conv 2-2/ BN / ReL	out_ channels =32, kernel_size =5, stride =2	32×252	2592
		Max Pooling	kernel_size =3, stride =1	32×250	/
		Conv 2-3/ BN / ReL	out_ channels =64, kernel_size =3, stride =2	64×124	6208
		Max Pooling	kernel_size =3, stride =1	64×122	/
		Conv 2-4/ BN / ReL	out_ channels =128, kernel_size =2, stride =2	128×61	16512
		Max Pooling	kernel_size =3, stride =1	128×59	/
	Channel 3	Conv 3-1/ BN / ReL	out_ channels =16, kernel_size =3, stride =2	16×511	64
		Max Pooling	kernel_size =5, stride =1	16×507	/
		Conv 3-2/ BN / ReL	out_ channels =32, kernel_size =2, stride =2	32×253	1056
		Max Pooling	kernel_size =5, stride =1	32×249	/
		Conv 3-3/ BN / ReL	out_ channels =64, kernel_size =1, stride =2	64×125	2112
		Max Pooling	ker _s=5, stride =1	64×121	/
		Conv 3-4/ BN / ReL	out_ channels =128, kernel_size =1, stride =2	128×61	8320
		Max Pooling	kernel_size =5, stride =1	128×57	/
SE attention	AvgPooling/Linear1/ReL/Linear2/Sigmoid		ratio=4	21120×1	1024
Subdomain adaptation	Linear1_S		out_features = 5096	5096×1	107632616
	Linear2_S		out_features = 1024	1024×1	5219328
Domain discrimination	Linear1_D		out_features = 2048	2048×1	43255808
	Linear2_D		out_features = 256	256×1	524544
	Linear3_D		out_features = 2	2×1	514
Classifier	Linear3		out_features = n_classes	n_classes×1	10250

as follows:

$$\begin{aligned}\hat{d}_H(p,q) &= \left\| \frac{1}{n_s}\sum_{i=1}^{n_s}\phi\left(x_i^s\right) - \frac{1}{n_t}\sum_{j=1}^{n_t}\phi(x_j^t) \right\|_H^2 \\ &= \frac{1}{n_s^2}\sum_{i=1}^{n_s}\sum_{j=1}^{n_s}k\left(x_i^s, x_j^s\right) + \frac{1}{n_t^2}\sum_{i=1}^{n_t}\sum_{j=1}^{n_t}k\left(x_i^t, x_j^t\right) \\ &\quad - \frac{2}{n_s n_t}\sum_{i=1}^{n_s}\sum_{j=1}^{n_t}k(x_i^s, x_j^t) \end{aligned} \tag{2}$$

where $k(\cdot,\cdot)$ is a Gaussian kernel function, which is generally chosen as Gaussian kernel.

III. THE PROPOSED FRAMEWORK

The proposed framework structure is shown in Fig. 2. The main idea of the proposed method is to fully extract the Domain-invariant features of the cross-domain unbalanced data and realize the global and subdomain self-adaptation of the cross-domain data. The following will be described in detail.

A. ADVERSARIAL UNSUPERVISED SUBDOMAIN ADAPTION MULTI-CHANNEL DEEP CONVOLUTIONAL NETWORKS

The proposed ASMDCN network framework consists of three modules: feature extractor, label classifier, and domain discriminator. The overall structure and detailed parameters of the model are shown in Table 1.

For the whole model, firstly, a multi-channel feature extractor is used to fully extract rich features from the multi-source labeled source domains and single-source unlabeled target domain, and the SE module is used to stimulate further and suppress the features to automatically obtain

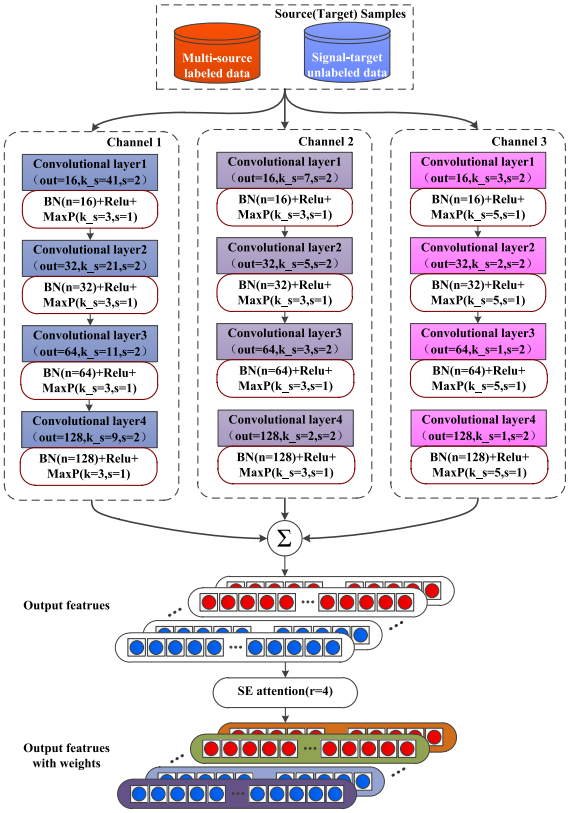

FIGURE 3. The structure of the designed feature extractor.

high-level features representations that are beneficial to model classification. Secondly, the features extracted from the source and target domains are sent to the label classifier to realize the classification of the source domain data and the subdomain adaptation of the cross-domain data. At the same time, the features are sent to the domain discriminator, and the source of the features is identified, which conducts the feature extractor to extract the domain-invariant features. Finally, under the optimization of the objective function, the model iteratively trains and updates the network parameters to achieve cross-domain unsupervised fault diagnosis of the target domain data. The components are described in detail below:

1) FEATURE EXTRACTOR G_f

Domain-invariant feature extraction of cross-domain data has always been a hot research topic. The typical approach is to apply a deeper network structure or a manually designed feature extraction algorithm to the signal. However, artificial feature extraction requires expert knowledge and experience to design according to task requirements or signal characteristics. In addition, with limited data, deep networks easily lead to overfitting, and the extracted features are not rich enough.

For the fault diagnosis problem of multi-source cross-domain with unbalanced data, the reasonable design of the feature extractor is one of the critical factors affecting the diagnosis performance. Inspired by references [6] and [32], we design a parallel three-channel feature extractor, as shown in Fig. 3, which comprises a four-layer ''convolution-pooling'' of three parallel branches. Channel 1 of the three parallel branches slides the convolution over the data using larger convolution kernels of size 41, followed by large convolution kernels of 21, 11, and 9 to fully capture the global high-level feature representation of the data. Channel 2 uses medium-sized convolution kernels 7, 5, 3, and 2, respectively, to extract local high-level feature representations of the data. Channel 3 uses a smaller convolution kernel to extract and locate critical features of the data. The structure and parameters of the three channels are the same, but the convolution kernel size is different. After each convolutional layer, the features are further processed using batch normalization and Relu to avoid gradient disappearance and explosion. Regarding channel dimension, the features obtained from the three channels are concatenated to get the output features. Then, SE attention is used to squeeze or excite the features further, and then the combined features with weight are obtained.

Specifically, assume that $x^{sn}(n = 1, 2, \ldots, N)$ and x^t ($x^{sn} \in \mathbb{R}^{N\times B\times L}, x^t \in \mathbb{R}^{B\times L}$) represent source domain data of N labeled working conditions of rolling bearings and unlabeled target domain data of single working conditions. B is the batch size of input data during model training, and L represents the length of data samples. Multi-source domains and single-target domain are input to the model for feature extraction.

The mapping function of the feature extractor composed of three branches is set as G_f. The mapping parameter is set as θ_f. Therefore, the i-th source domain x_i^{sn} sample and the j-th target domain x_j^t sample are input to G_f. The features obtained from the three channels are concatenated to obtain the high-level feature representation $\tilde{Z}^s = G_f(x^{sn}; \theta_f)$ and $\tilde{Z}^t = G_f(x^t; \theta_f)(\tilde{Z}^s, \tilde{Z}^t \in \mathbb{R}^{B\times D})$, where D is the number of channels of the feature map output by the feature extractor. Then, the resulting features $\tilde{Z}^s$ and $\tilde{Z}^t$ are sent to SE attention for further processing. Refer to the design idea of channel attention mechanism in literature [32]. It comprises a global average pooling (GAP) layer, two fully-connected (FC) layers, a ReLU activation function, and a Sigmoid activation function. Features $\tilde{Z}^s$ and $\tilde{Z}^t$ are first reduced in dimension by GAP and then ascended dimension by linear layer to obtain attention weight $\omega_{s/t} = \sigma\{FC[ReLU(FC(\tilde{Z}^{s/t}))]\}$, where $\sigma(\cdot) = 1/(1 + e^{-x})$ is the Sigmoid function, and $FC(\cdot)$ is a linear transformation. Finally, we get the features $Z^s = \omega_s \cdot \tilde{Z}^s$ and $Z^t = \omega_t \cdot \tilde{Z}^t$ with attention weights.

2) DOMAIN DISCRIMINATOR G_d

Due to the different production processes, the operating conditions of rolling bearings need to be changed frequently, which leads to the difference in the distribution of data collected under various working conditions. We employ the domain adversarial adaption loss function to reduce global distribution differences.

The domain discriminator is composed of three linear layers. After the first two linear layers, the Relu activation function is used to realize nonlinear transformation, and the last layer uses the Softmax activation function. In the training process of ASMDCN, feature extractor G_f and domain discriminator G_d (θ_d is the parameter of the learning process) play an antagonistic role, and the two form a maximum and minimum game.

Specifically, as shown in Fig. 2, we add a gradient reversal layer with parameter μ between G_f and G_d to solve the game problem. The feature extractor G_f expects the domain discriminator G_d to be unable to distinguish the source of the extracted features through continuous learning. In contrast, the domain discriminator G_d expects to identify whether the features belong to the source or target domain through training. Therefore, in the data of a training batch, the objective function of the domain against loss is as follows:

$$L_{AD} = \frac{1}{B}\sum_{i=1}^{B} log(G_d(G_f(x_i^{sn};\theta_f));\theta_d) + \frac{1}{B}\sum_{i=1}^{B} log(1 - G_d(G_f(x_i^{t};\theta_f));\theta_d) \quad (3)$$

3) LABEL CLASSIFIER G_l

In previous studies, people usually constructed a balanced dataset to train the model and used the cross-entropy loss function as the optimization target of the source domain classifier. However, the data collected in actual production is usually unbalanced because the equipment is generally healthy. Hence, the data collected are primarily healthy samples; the fault samples account for less. If the cross-entropy function is directly used as the optimization target, the model will not learn enough for a few samples and cannot achieve accurate classification.

For the processing of unbalanced data, Lin et al. [33] proposed a focal loss (FL) function in 2018, which could adjust the weight values of samples of different categories and samples with varying classification difficulties and achieve great success. Subsequently, FL and its variants achieved remarkable results in applying bearing fault diagnosis [34], [35]. Inspired by the above ideas, we design a new classification loss function for unbalanced data based on cross-entropy with dynamic weights and improved Focal loss. In the design, we consider two fundamental problems: the classification difficulty of input samples and the imbalance of sample categories. The calculation formula of the designed objective function is as follows:

$$L_{w-f} = \frac{1}{B}\sum_{i=1}^{B}\sum_{j=1}^{C}(1 - p(y_i^s = j|Z_i^s))^{\gamma} \cdot w_c^s \cdot (-log(p(y_i^s = j|Z_i^s))) \quad (4)$$

where $p(y_i^s = j|Z_i^s)$ is the probability that the feature of the i-th sample in the source domain is predicted to be of class C, and j is the actual label of this sample. γ is a hyperparameter. w_c^s is the weight corresponding to the cross-entropy loss function in the model training process, and its calculation formula is as follows:

$$w_c^s = \frac{1}{log(\mu + n_c/N)}, c \in \{1, 2, \ldots, n\_class\} \quad (5)$$

where μ is the hyperparameter, n_c is the sum of labels belonging to class c in the current BATCH, N is the total number of samples in the current BATCH, and $n_class$is the total number of categories.

According to the characteristics of the data collected by the rolling bearing, $(1 - p(y_i^s = j|Z_i^s))^{\gamma}$ in the objective function L_{w-f} is used to control the classification difficulty of the input samples of the model. A more significant loss value is assigned to the samples that are difficult to classify, and the opposite value is set to the samples that are easy to classify. Since each BATCH of data input gives a different number of classes to the model, w_c^s is used to assign dynamic weights to the cross-entropy loss function within each batch to deal with sample class imbalance. Compared with the weight coefficient of ordinary class weighting calculation, even if the number of samples n_c of a specific class participating in training in the current BATCH is 0, its weight parameters are bounded, effectively avoiding the loss value disappearing.

The domain discriminator G_d mentioned above can induce the feature extractor G_f to extract domain invariant features by reducing the global distribution difference of cross-domain data. Still, it ignores the fine-grained information of the data. To solve this problem, LMMD is introduced to do further subdomain alignment on the features obtained from the source and target domains. LMMD is weighted according to MMD, which considers the weight of the sample according to the category of the sample, which can be expressed as follows:

$$L_{LMMD}(p, q) = \frac{1}{N}\sum_{n=1}^{N}\left\| \sum_{x_i^s \in X_s} w_i^{sn}\phi(x_i^s) - \sum_{x_j^t \in X_t} w_j^{tn}\phi(x_j^t) \right\|_H^2 \quad (6)$$

where w_i^{sn} and w_j^{tn} represent the weights of x_i^s and x_j^t belonging to category n, respectively. N is the number of sample classes. In a BATCH, $\sum_{i=1}^{n_s} w_i^{sn} = 1$ and $\sum_{j=1}^{n_t} w_j^{tn} = 1$. For a given sample x_i, w_i^n can be calculated as follows:

$$w_i^n = \frac{y_{in}}{\sum_{(x_j, y_j)\in D} y_{jn}} \quad (7)$$

where y_{in} is the label of H_i and the n-th element of vector y_n. For the source domain sample x_i^s, we can calculate w_i^n by its actual label y_{in}. However, the target domain sample x_j^t is unlabeled. Considering that the output feature H^t of the subdomain alignment module can be converted into a probability distribution, we use its predicted pseudo-label $\hat{y}_{jn}^t$ to calculate the weight w_j^n of the target domain. According to Fig. 1, H^s and H^t(H^s, $H^t \in \mathbb{R}^{B\times n}$) are the output features of the first linear layer in the LMMD embedded source domain

classifier and subdomain alignment module. We can derive an adaption function for subdomain alignment:

$$L_{LMMD}\left(H^s, H^t\right) = \left\| \frac{1}{n_s}\sum_{i=1}^{n_s} w_i^{sn}\phi\left(H_i^s\right) - \frac{1}{n_t}\sum_{j=1}^{n_t} w_j^{tn}\phi(H_j^t) \right\|_H^2$$
$$= \frac{1}{N}\sum_{n=1}^{N}\left[\sum_{i=1}^{n_s}\sum_{j=1}^{n_s} w_i^{sn}w_j^{sn}k\left(H_i^s, H_j^s\right) + \sum_{i=1}^{n_t}\sum_{j=1}^{n_t} w_i^{tn}w_j^{tn}k\left(H_i^t, H_j^t\right) - 2\sum_{i=1}^{n_s}\sum_{j=1}^{n_t} w_i^{sn}w_j^{tn}k(H_i^s, H_j^t)\right] \quad (8)$$

In summary, we can get the loss function of the label classifier:

$$L_l = L_{w-f} + \lambda L_{LMMD}\left(H^s, H^t\right) \quad (9)$$

where λ is the compromise parameter of subdomain adaption and classification loss, the formula is as follows:

$$\lambda = \frac{2}{1+e^{-10m/M}} - 1 \quad (10)$$

where m is the current epoch, and M is the total epochs.

B. TRAINING PROCESS OF ASMDCN

According to the above, the proposed objective optimization function of ASMDCN consists of the following three parts:

1) Source domain classifier error
2) Domain discriminator error
3) Subdomain adaption error

Therefore, combined with (3) and (9), the overall objective optimization function of ASMDCN is:

$$L_{total}(\theta_f, \theta_c, \theta_d) = L_{w-f} + \lambda L_{LMMD}\left(H^s, H^t\right) - \mu L_{AD} \quad (11)$$

where μ is the tradeoff parameter of L_{total}.

The three parts of L_{total} each play different optimization roles. First of all, L_{w-f} is designed with full consideration of difficult samples and highly unbalanced data in the source domain data. In the ASMDCN training process, the parameter θ_f of G_f is updated by minimizing the L_{w-f} function to achieve high-accuracy classification of the source domain. Secondly, $L_{LMMD}\left(H^s, H^t\right)$ is an optimization function that aligns the related subdomains of the target and source domains. With the help of the source domain classifier, the accurate classification of the target domain without labels can be achieved by minimizing $L_{LMMD}\left(H^s, H^t\right)$. Finally, L_{AD} is the optimization objective function of adversarial learning. In the ASMDCN model, G_f and G_d are regarded as a minimax two-person game, and the performance of G_f and G_d is improved in the adversarial process. Specifically, optimizing the parameter θ_f of G_f minimizes the L_{w-f} function to confuse the two domains so that G_f can learn the domain invariant features. At the same time, by optimizing the parameter θ_d of L_{AD}, the L_{AD} function is maximized to improve the discriminant ability of the domain discriminator.

For all diagnostic tasks, we use SGD with a momentum of 0.9 as the network optimizer. In the process of network iterative training, the learning rate η_θ is constantly updated. $\eta_\theta = \eta_0/(1+\alpha\theta)^\beta$,where θ is the training progress linearly changing from 0 to 1, $\eta_0 = 0.001, \alpha = 10$, and $\beta = 0.75$ [27]. Total epochs are 300, batch size is 64, weight_decay is 5e-4. The network training process adopts the early-stopping strategy, and the stopping cycle is 30. Detailed training strategy are shown in Table 2.

TABLE 2. Training strategy of ASMDCN.

Algorithm：training strategy for the proposed ASMDCN

1)Require and initialization：

Input multi-source domain data： $D_s = \{\{(x_i^{s1}, y_i^{s1})\}_{i=1}^{n_{s1}}, \text{L}, \{(x_i^{sn}, y_i^{sn})\}_{i=1}^{n_{sn}}\}$ and target domain data: $D_t = \{(x_j^t)\}_{j=1}^{n_t}$. Initialize the parameters q_f, q_c, q_d ,feature extractor G_f ,label classifier G_l ,domain discriminator G_d .batch size is B. Learning rate is h_q .

2)Training process

for each epoch do:

Forward propagation

random samples $x_s = \{(x_i^{sn})\}(i = 1,\text{L},B, n = 1,\text{L},N)$, $x_t = \{(x_j^t)\}$ $(j = 1,\text{L},B)$ calculate features $Z^s = G_f(x^{sn};\theta_f)$ and $z^t = G_f(x^t;\theta_f)$, H^s and H^t , class label $\hat{y}_l^s = G_l(Z^s;q_c)$ and $\hat{y}_l^t = G_l(Z^t;q_c)$, domain label $\hat{y}_d^s = G_d(Z^s;q_d)$ and $\hat{y}_d^t = G_d(Z^t;q_d)$.

Propagation back

calculate the source domain classifier loss L_{w-f} using Eq.4, LMMD loss L_{LMMD} using Eq.8, domain discriminator loss L_{AD} using Eq.3, and total loss L_{total} using Eq.11.

Update the parameters q_f, q_c, q_d

$$q_f \neg q_f - h_q\left(\frac{\partial L_{w-f}}{\partial q_f} + l\frac{\partial L_{LMMD}}{\partial q_f} - m\frac{\partial L_{AD}}{\partial q_f}\right)$$
$$q_c \neg q_c - h_q\left(\frac{\partial L_{w-f}}{\partial q_c} + l\frac{\partial L_{LMMD}}{\partial q_c}\right)$$
$$q_d \neg q_d - h_q\frac{\partial L_{AD}}{\partial q_d}$$

end

3)Testing

Save all parameters of the model, and predict unlabeled target domain samples.

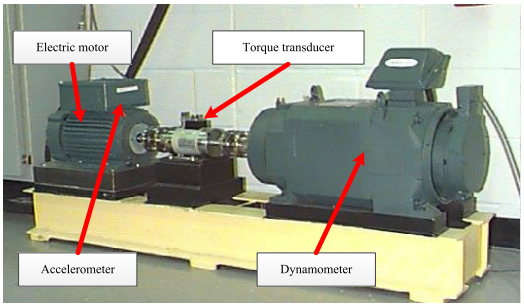

FIGURE 4. Bearing experimental platform of CWRU.

TABLE 3. Description of imbalanced dataset for CWRU.

Type	Training set			Testing set
	Dataset a	Dataset b	Dataset c	
Normal	100	100	100	40
IR007 (7mil)	30	20	15	40
OR007 (7mil)	30	20	15	40
B007(7mil)	30	20	15	40
IR0014(14mil)	25	15	10	40
OR014(14mil)	25	15	10	40
B014 (14mil)	25	15	10	40
IR021 (21mil)	20	10	6	40
OR021(21mil)	20	10	6	40
B021(21mil)	20	10	6	40

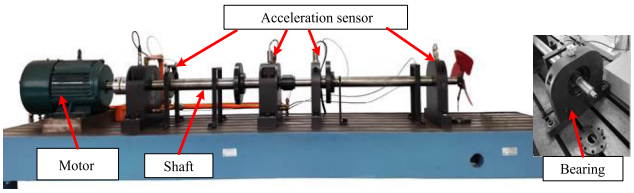

FIGURE 5. Bearing experimental platform of Hou De.

TABLE 4. Description of the imbalanced dataset for case 2.

Type	Training set			Testing set
	Dataset a	Dataset b	Dataset c	
Normal	150	150	150	80
Ball fault	50	30	20	80
Fix fault	50	30	20	80
Inner Race fault	50	30	20	80
Outer Race fault	50	30	20	80

IV. EXPERIMENTAL RESULTS AND VERIFICATIONS

In this section, datasets from Case Western Reserve University (CWRU) and Wuxi Hou De Automation Instrument Co., LTD. (Hou De) are selected to verify the migration diagnostic performance of the proposed method and the stability of processing unbalanced data. Regarding comparison methods, we chose the currently popular DANN [36], D-Coral [37], DDC [38], DSAN [27], DCTLN [39], DASAN [28] and other methods for comparison. We use the PyTorch framework to build the network model.

A. INTRODUCTION OF DATASET

1) CWRU BEARING DATASET

As shown in Fig. 4, the test bench comprises an induction motor, an accelerometer, a torque converter and a dynamometer. This dataset is the most commonly used in rolling bearing fault diagnosis because of its rich fault types and high data quality. In this experiment, we selected vibration signals with a sampling frequency of 12K from the drive end bearing, which were collected under motor loads of 0, 1, 2 and 3 HP, respectively. There are four health status signals: normal, inner ring fault, outer ring fault and rolling element fault. Among them, each fault signal is divided into three faults of different severity, according to the damage diameter of the bearing (7mil, 14mil, and 21mil). Therefore, we regard the four motor loads as operating conditions (A, B, C, D), and ten health status signals can be obtained under each working condition.

The failure of rolling bearings in industrial field service has a specific rule: under normal circumstances, it first works in a normal state, then a slight fault occurs, then gradually develops to a moderate fault, and finally enters a serious fault state until the equipment is shut down. Therefore, the number of vibration signals obtained at each stage of the failure process is different. To be closer to practical engineering applications and reflect the superiority of our proposed model, we established unbalanced datasets, as shown in Table 3., according to the severity of faults and the number of samples obtained, in which the length of each sample is 1024.

The number of samples in the test set is 40. It is worth mentioning that datasets need to be established for the above four working conditions according to the number of samples in Table 3.

2) HOU DE BEARING DATASET

As shown in Fig. 5, this test bench comprises a motor, shaft, acceleration sensor and rolling bearing. It has a simple structure, convenient operation, stable running state and high data quality. On this bench, we simulated five operating states with four speeds of 2600, 2800, 3000 and 3200r/min, respectively: normal, rolling element fault, cage fault, inner ring fault and outer ring fault. The signal sampling frequency is 8K. We regard each speed as an operating condition, so there are four operating conditions (A, B, C, D), and each working condition has five operating states.

For the data collected by this experimental platform, we also built the dataset shown in Table 4. Similar to the case, the length of each sample in the dataset is also 1024, and the dataset should also be made by Table 4 for four operating conditions. We also set up four transfer diagnosis tasks (A/B/C→ D, A/B/D → C, A/C/D→ B, D/B/C → A).

B. COMPARATIVE METHODS

To comprehensively evaluate the superiority and effectiveness of the proposed transfer learning method, we select the transfer learning strategy with good performance to carry out comparative experiments. The comparison method is described in detail as follows:

1) DANN

The basic structure of the DANN is composed of a feature extractor, label classifier and domain discriminator. The feature distribution difference between the source and target domains is reduced by adversarial training. Then, the two domains are confused to make the model learn the invariant features.

2) D-CORAL

It utilized the convolution/pooling layer to extract data features and embedded the correlation alignment into the fully

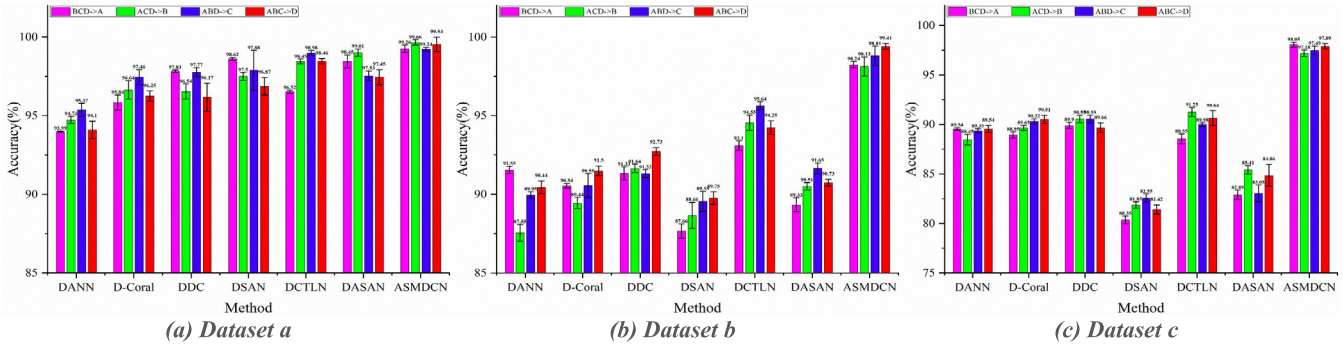

(a) Dataset a (b) Dataset b (c) Dataset c

FIGURE 6. Transfer diagnosis accuracy of CWRU on the different datasets.

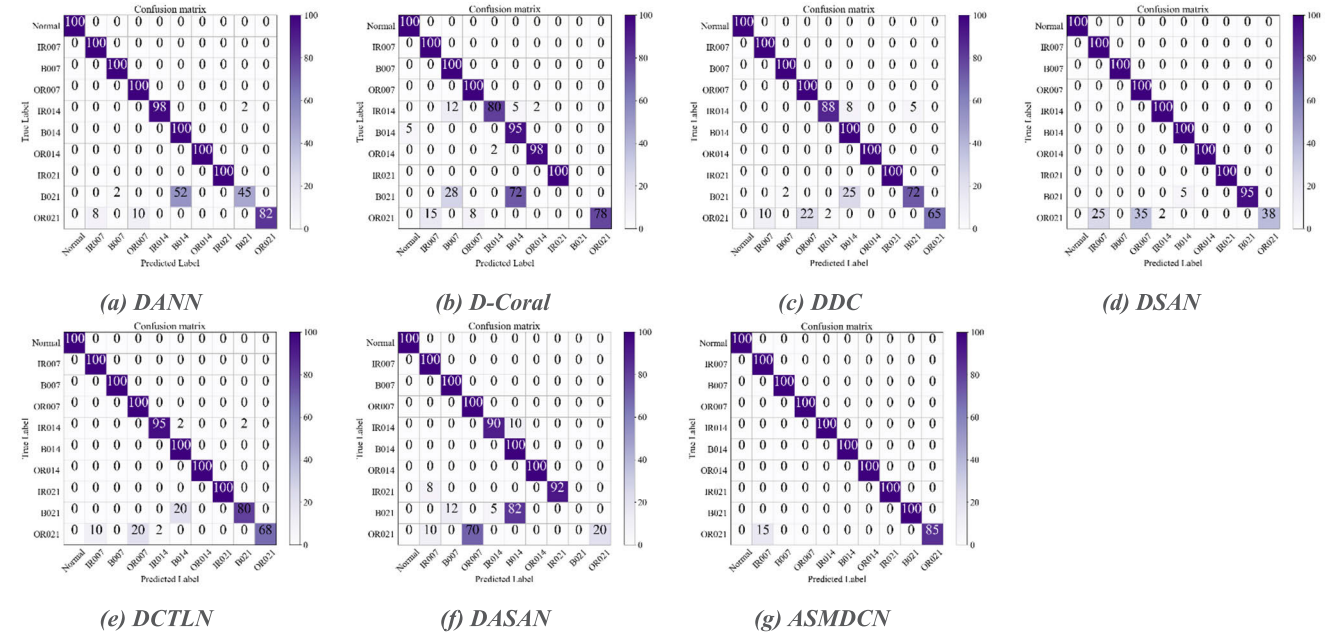

(a) DANN (b) D-Coral (c) DDC (d) DSAN

(e) DCTLN (f) DASAN (g) ASMDCN

FIGURE 7. Confusion matrix of different methods on the dataset c in task A/B/C→D for CWRU.

connected layer as second-order moment matching to reduce the difference in feature distribution between the two domains to achieve domain self-adaptation

3) DDC

It used MMD in the fully connected layer of the network model to reduce the global distribution difference between the two domains and learned features through iterative training.

4) DSAN

Similar to DDC. The difference is that LMMD is used in the fully connected layer of the model further to align the related subdomains of the two domains.

5) DCTLN

In essence, it is a convolutional transfer learning network that reduces the difference between the feature distributions extracted by the feature extractor through domain adversarial training and then maximizes the consistency of the global feature distribution by using MMD.

6) DASAN

Similar to DCTLN, DASAN focuses on global adaptation and realizes subdomain adaptation.

The ASMDCN proposed in this paper is similar to DASAN. However, DASAN assumes the dataset is balanced, and the label classifier adopts cross-entropy. However, ASMDCN considers the problem that data categories are usually unbalanced in engineering practice and designs L_{w-f} that can handle unbalanced data. In addition, we use multiple source domain data instead of single source domain data during model training.

It is worth noting that the above comparative methods use different network architectures. When compared directly with ASMDCN, the diagnosis is not convincing. Therefore, to ensure a fair comparison of migration results, we designed

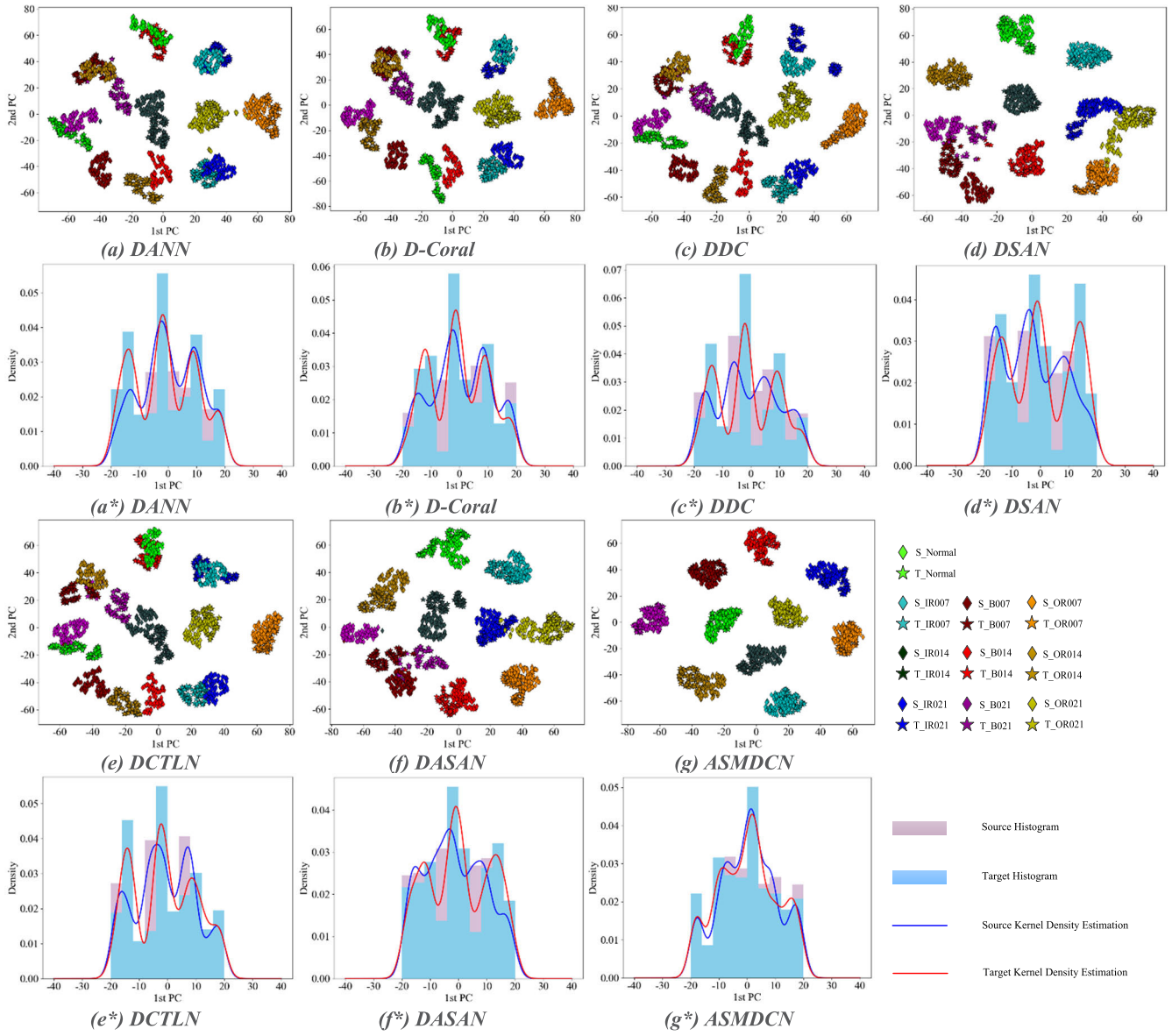

FIGURE 8. Seven methods for data visualization of transfer diagnostic task A/B/C→D on the dataset c.

the model architecture of the above comparison method to be the same as that of ASMDCN. That is, the feature extractor, label classifier, and domain discriminator have the same parameters [40].

C. EXPERIMENTAL RESULTS FOR CWRU

We employ labeled multi-source domain data and unlabeled single target domain to train the diagnostic model in this experiment. According to the four operating conditions of the testing sets, we set a total of four transfer diagnosis tasks (A/B/C→ D, A/B/D → C, A/C/D→ B, D/B/C → A). We used the classification accuracy of test data from 4 conditions (including three source conditions and one target condition) to evaluate the diagnostic performance of the model, which is worth noting. We performed all transfer diagnosis results ten times to ensure the influence of random initialization on network parameters. The transfer diagnosis results of the proposed ASMDCN and six transfer learning comparative methods for CWRU datasets are shown in Fig. 6.

The diagnosis results in Fig. 6(a) were carried out under a slightly unbalanced dataset. The diagnostic accuracy was the lowest since DANN only adopted an adversarial training strategy and ignored cross-domain data alignment. The methods of D-Coral and DDC only align the global cross-domain data, and the diagnostic accuracy is also low. DSAN uses LMMD to realize global alignment of cross-operating data with related subdomains, resulting in slightly higher diagnostic accuracy than D-Coral and DDC. Although DCTLN adopts the domain adaption method, it only employs MMD to align cross-domain data from a global perspective. It ignores

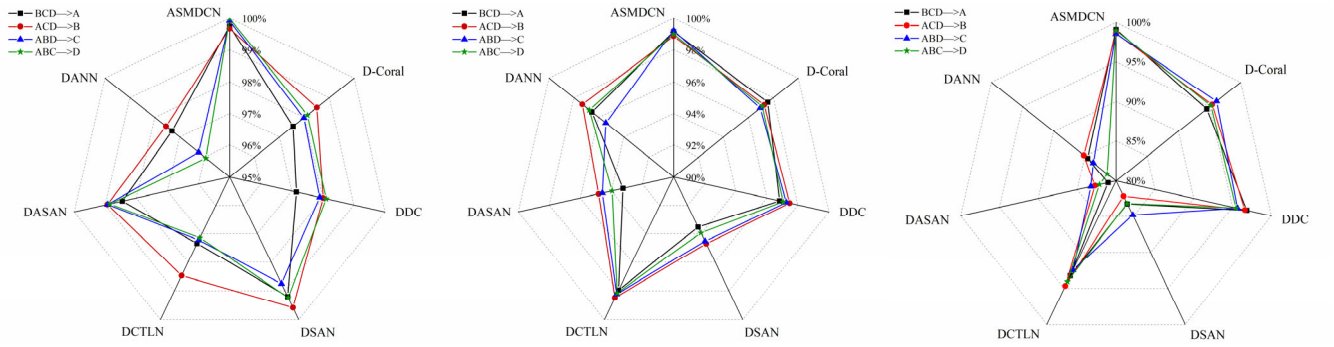

(a) Dataset a *(b) Dataset b* *(c) Dataset c*

FIGURE 9. Transfer diagnosis accuracy of Hou De on the different datasets.

TABLE 5. The diagnostic accuracy of ASMDCN for each working condition under the three methods for CWRU.

Model	A	B	C	D
Method1	98.71±0.413	88.19±1.482	90.13±1.174	98.61±0.498
Method2	97.99±0.265	97.58±0.357	89.94±0.688	98.19±0.376
Method3	97.28±0.254	98.03±0.353	97.82±0.236	98.43±0.217

TABLE 6. The diagnostic accuracy of ASMDCN for each working condition under the three methods for Hou De.

Model	A	B	C	D
Method1	99.73±0.127	97.51±0.989	79.40±1.636	72.69±1.397
Method2	99.40±0.566	97.71±1.359	97.78±0.820	85.13±1.654
Method3	99.90±0.167	97.85±0.827	98.74±0.532	97.71±0.334

further processing of related subdomains, resulting in low diagnostic accuracy. The DSAN method comprehensively uses domain adaption strategy and LMMD to somewhat improve its diagnostic accuracy. Still, this method ignores the influence of unbalanced data on the model, making its diagnostic accuracy lower than the proposed ASMDCN. Moreover, with increased data categories' imbalance, the diagnostic accuracy of the comparative methods showed a downward trend. (b) and (c) in Fig. 6 are obtained under moderately and severely unbalanced datasets, respectively. The diagnostic accuracy of DSAN and DASAN methods is seriously decreased because these two methods ignore the influencing factors of unbalanced data and pay too much attention to subdomain adaptation. While the other methods mainly learn the global features, there is no overfitting phenomenon, but the diagnostic accuracy also shows a trend of decline. On the contrary, the proposed ASMDCN has the highest diagnostic accuracy among the three datasets because it utilizes a function L_{w-f} that can handle unbalanced data, and employs domain adversarial and LMMD training strategies. Although. The diagnostic accuracy of ASMDCN decreased with the aggravation of data imbalance, but the lowest diagnostic accuracy still reached 97.18%.

To more clearly show the experimental results of the proposed ASMDCN and the comparison method, we plot the confusion matrix for the diagnosis results of the transfer diagnosis task A/B/C→D in the case of dataset c. As shown in Fig. 7, the horizontal coordinate represents the labels diagnosed by the model, the vertical coordinate represents the actual labels and the numbers on the diagonal represent the percentage of correctly classified labels. We can see from the figure that the proposed method has the highest diagnostic accuracy. The classification errors of the four comparison methods, DANN, D-Coral, DDC and DCTLN, are mainly concentrated in moderate and severe faults. In contrast, DSAN and DASAN are primarily focused on severe faults. Meanwhile, the above seven comparison methods can correctly classify normal and minor faults. The above results are because the number of samples participating in model training is unbalanced, resulting in the model learning more fully for most samples but not enough for a few samples.

To display the above experimental results more intuitively, we utilize t-SNE to visualize the characteristics of the test data. The high-dimensional features are reduced into two-dimensional features and one-dimensional features. Next, we employ two-dimensional features to draw cluster graphs (represented by ($\times$)) and one-dimensional features to draw histograms and probability distribution function curves (represented by ($\times*$)). As can be seen from Fig. 8, the cluster graph of the proposed ASMDCN method gathers the same type of features in the source domain and the target domain together well, and the classification among various fault data is obvious. Also, the data distribution difference between the source and target domains is slight in the combined graph. On the contrary, the visualization effect of the contrast method is poor.

In addition, we use a different number of source domains to train the model to verify the idea that using multi-source domain data can enhance the model's generalization performance. It is worth noting that the experiments in this part are carried out in the case of dataset c, and we separately calculate the diagnostic accuracy of the test data under various working conditions. Details of the experiment are as follows:

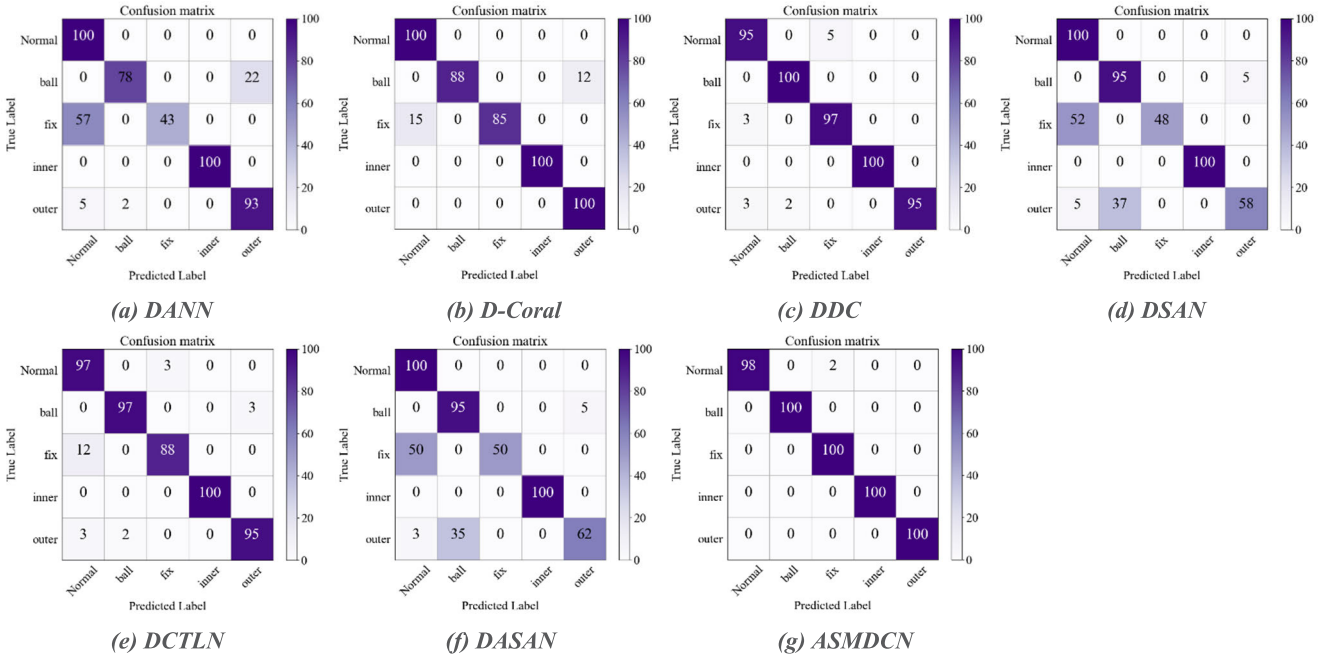

FIGURE 10. Confusion matrix of different methods on the dataset c in task A/C/D→B for Hou De.

1) METHOD 1

We use labeled condition A as the source domain and unlabeled condition D as the target domain to train the network model.

2) METHOD 2

Labeled working conditions A and B are used as the source domain, and working condition D is used as the target domain.

3) SEND THEM TO THE MODEL FOR TRAINING

4) METHOD 3

We use three labeled working conditions, A, B, and C, as the source domain and unlabeled working condition D as the target domain, as the input data of the network model for training.

We also conducted ten experiments, and the diagnostic accuracy of the three methods is shown in Table 5. For method 1, we can see that the model has low test accuracy for conditions B and C. In contrast, high diagnostic accuracy for conditions A and D. Similarly, the model of method 2 has a lower test accuracy for working condition C but a high diagnostic accuracy for other working conditions. On the contrary, method 3 has higher recognition accuracy for all working conditions. The above results are because method 1 uses only working conditions A and D, method 2 uses working conditions A, B and D, and method 3 uses all working conditions comprehensively. Therefore, we should fully exploit the source domain data to train the model to strengthen its generalization ability.

D. EXPERIMENTAL RESULTS FOR HOU DE

We conducted experiments in the Hou De laboratory to verify the model's generalization performance on different datasets further. In this experiment, the details of our experiment are the same as those of the CWRU experiment. We also set up four transfer diagnosis tasks (A/B/C→D, A/B/D→C, A/C/D→B, D/B/C→A). Source domains from three conditions and a single-condition target domain were used to train the model, the model's classification accuracy was tested by the testing set, and all the transfer diagnosis results were performed ten times. The experimental results are shown in Fig. 9. As can be seen, the model trained by ASMDCN under the three datasets has the highest diagnostic accuracy for the testing set. As the increase of the unbalance of data categories, the diagnostic accuracy of the other six comparative methods decreases to varying degrees. In other words, we can get similar conclusions to CWRU under this experiment.

In this experiment, to visualize the diagnostic results more clearly, as shown in Fig. 9, we trained the model of ASMDCN and the comparative methods in the case of dataset c by the transfer diagnostic task A/C/D→B. We drew the confusion matrix of the testing set diagnostic results. Simultaneously, in the same case, as shown in Figure 10, we also draw the cluster graphs and probability distribution function curves to visualize the diagnosis results further. It can be seen from FIG. 9 and FIG. 10 that the diagnostic effect of the proposed method is optimal.

Finally, similar to the experimental details of CWRU, we also trained the network model with a different number of source domains and diagnosed the testing set for all conditions ten times. All experiments were conducted

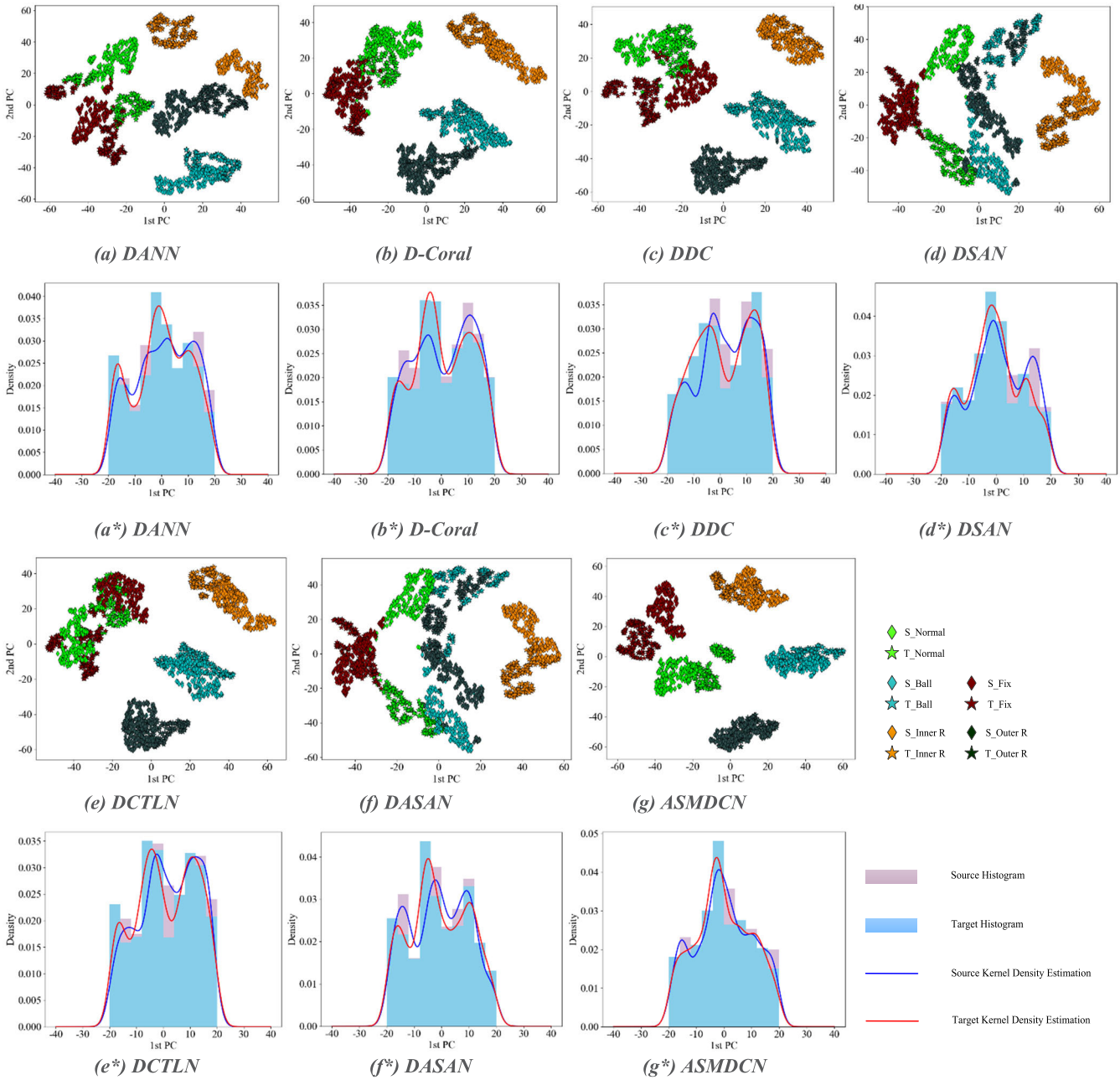

FIGURE 11. Confusion matrix of different methods on the dataset c in task A/C/D→B for Hou De.

with dataset c, and the comparative Method1, Method2, and Method3 used labeled source domain conditions A, A/C, and A/C/D, respectively, and target domain conditions B. The diagnosis results are shown in Table 6. The results again verify that training multi-source domain data can improve the network model.

E. LIMITATION DISCUSSION

Although the proposed ASMDCN in this paper achieved the highest diagnostic accuracy, the method still has the following limitations.

1) The proposed three-channel feature extraction modules all use 4-layer convolution/pooling and have many network parameters, which wastes computing resources to a certain extent.

2) The proposed loss function contains two hyperparameters, which must be set according to the number of samples involved in model training.

3) Although ASMDCN can realize the task of cross-operating unsupervised fault diagnosis of rolling bearings affected by unbalanced data. However, through many experiments, it is found that with the increase of sample imbalance,

the diagnostic accuracy of the proposed method also gradually decreases, resulting in the final diagnosis failure.

V. CONCLUSION

This paper proposed a cross-operating unsupervised intelligent diagnosis method for rolling bearings called ASMDCN. A novel loss function is designed, which can effectively train the model with unbalanced data of a multi-source domain and a single target domain, realizing the high-precision diagnostic decision of the testing set. In addition, under the joint constraints of adversarial training strategy and subdomain adaptive, the model can promote the parallel multi-channel feature extractor to fully mine domain-invariant features under multiple working conditions, providing a new perspective for intelligent fault diagnosis based on domain generalization. We verify the validity and generalization of the ASMDCN on multiple transmission diagnostic tasks of 2 datasets. The superiority of the ASMDCN is proved by comparing it with the current popular methods.

REFERENCES

[1] H. Wang, Z. Liu, D. Peng, and Z. Cheng, "Attention-guided joint learning CNN with noise robustness for bearing fault diagnosis and vibration signal denoising," *ISA Trans.*, vol. 128, pp. 470–484, Sep. 2022, doi: 10.1016/j.isatra.2021.11.028.

[2] Y. Sun, J. Wang, and X. Wang, "Fault diagnosis of mechanical equipment in high energy consumption industries in China: A review," *Mech. Syst. Signal Process.*, vol. 186, Mar. 2023, Art. no. 109833, doi: 10.1016/j.ymssp.2022.109833.

[3] H. Shao, M. Xia, G. Han, Y. Zhang, and J. Wan, "Intelligent fault diagnosis of rotor-bearing system under varying working conditions with modified transfer convolutional neural network and thermal images," *IEEE Trans. Ind. Informat.*, vol. 17, no. 5, pp. 3488–3496, May 2021, doi: 10.1109/TII.2020.3005965.

[4] J. Tian, D. Han, M. Li, and P. Shi, "A multi-source information transfer learning method with subdomain adaptation for cross-domain fault diagnosis," *Knowl.-Based Syst.*, vol. 243, May 2022, Art. no. 108466, doi: 10.1016/j.knosys.2022.108466.

[5] C. Zhao and W. Shen, "Adversarial mutual information-guided single domain generalization network for intelligent fault diagnosis," *IEEE Trans. Ind. Informat.*, vol. 19, no. 3, pp. 2909–2918, Mar. 2023, doi: 10.1109/TII.2022.3175018.

[6] T. Huo, L. Deng, B. Zhang, J. Gong, B. Hu, R. Zhao, and Z. Liu, "Novel imbalanced subdomain adaption multiscale convolutional network for cross-domain unsupervised fault diagnosis of rolling bearings," *Meas. Sci. Technol.*, vol. 35, no. 1, Jan. 2024, Art. no. 015905, doi: 10.1088/1361-6501/ad006a.

[7] E. Zio, "Prognostics and health management (PHM): Where are we and where do we (need to) go in theory and practice," *Rel. Eng. Syst. Saf.*, vol. 218, Feb. 2022, Art. no. 108119, doi: 10.1016/j.ress.2021.108119.

[8] Y. Xiao, H. Shao, J. Wang, S. Yan, and B. Liu, "Bayesian variational transformer: A generalizable model for rotating machinery fault diagnosis," *Mech. Syst. Signal Process.*, vol. 207, Jan. 2024, Art. no. 110936, doi: 10.1016/j.ymssp.2023.110936.

[9] R. Yan, Z. Shang, H. Xu, J. Wen, Z. Zhao, X. Chen, and R. X. Gao, "Wavelet transform for rotary machine fault diagnosis:10 years revisited," *Mech. Syst. Signal Process.*, vol. 200, Oct. 2023, Art. no. 110545, doi: 10.1016/j.ymssp.2023.110545.

[10] S. Buchaiah and P. Shakya, "Bearing fault diagnosis and prognosis using data fusion based feature extraction and feature selection," *Measurement*, vol. 188, Jan. 2022, Art. no. 110506, doi: 10.1016/j.measurement.2021.110506.

[11] L. Xu, S. Chatterton, and P. Pennacchi, "Rolling element bearing diagnosis based on singular value decomposition and composite squared envelope spectrum," *Mech. Syst. Signal Process.*, vol. 148, Feb. 2021, Art. no. 107174, doi: 10.1016/j.ymssp.2020.107174.

[12] H. Shao, X. Zhou, J. Lin, and B. Liu, "Few-shot cross-domain fault diagnosis of bearing driven by task-supervised ANIL," *IEEE Internet Things J.*, early access, Jan. 31, 2024, doi: 10.1109/jiot.2024.3360432.

[13] Z. Zhu, Y. Lei, G. Qi, Y. Chai, N. Mazur, Y. An, and X. Huang, "A review of the application of deep learning in intelligent fault diagnosis of rotating machinery," *Measurement*, vol. 206, Jan. 2023, Art. no. 112346, doi: 10.1016/j.measurement.2022.112346.

[14] D. Yang, W. Zhang, and Y. Jiang, "Mechanical fault diagnosis based on deep transfer learning: A review," *Meas. Sci. Technol.*, vol. 34, no. 11, Nov. 2023, Art. no. 112001, doi: 10.1088/1361-6501/ace7e6.

[15] Y. Ge, F. Zhang, and Y. Ren, "Adaptive fault diagnosis method for rotating machinery with unknown faults under multiple working conditions," *J. Manuf. Syst.*, vol. 63, pp. 177–184, Apr. 2022, doi: 10.1016/j.jmsy.2022.03.009.

[16] B. Hu, J. Liu, R. Zhao, Y. Xu, and T. Huo, "A new fault diagnosis method for unbalanced data based on 1DCNN and L2-SVM," *Appl. Sci.*, vol. 12, no. 19, p. 9880, Sep. 2022, doi: 10.3390/app12199880.

[17] Y. Zhang, T. Zhou, X. Huang, L. Cao, and Q. Zhou, "Fault diagnosis of rotating machinery based on recurrent neural networks," *Measurement*, vol. 171, Feb. 2021, Art. no. 108774, doi: 10.1016/j.measurement.2020.108774.

[18] K. Zhao, F. Jia, and H. Shao, "A novel conditional weighting transfer Wasserstein auto-encoder for rolling bearing fault diagnosis with multi-source domains," *Knowl.-Based Syst.*, vol. 262, Feb. 2023, Art. no. 110203, doi: 10.1016/j.knosys.2022.110203.

[19] X. Zhao, J. Yao, W. Deng, P. Ding, J. Zhuang, and Z. Liu, "Multi-scale deep graph convolutional networks for intelligent fault diagnosis of rotor-bearing system under fluctuating working conditions," *IEEE Trans. Ind. Informat.*, vol. 19, no. 1, pp. 166–176, Jan. 2023, doi: 10.1109/TII.2022.3161674.

[20] Z. Xing, R. Zhao, Y. Wu, and T. He, "Intelligent fault diagnosis of rolling bearing based on novel CNN model considering data imbalance," *Appl. Intell.*, vol. 52, no. 14, pp. 16281–16293, Nov. 2022, doi: 10.1007/s10489-022-03196-x.

[21] W. Zhang, D. Chen, and Y. Xiao, "A novel fault diagnosis method based on semisupervised contrast learning," in *Proc. IEEE Int. Conf. Prognostics Health Manage. (ICPHM)*, Detroit (Romulus), MI, USA, Jun. 2022, pp. 82–87, doi: 10.1109/ICPHM53196.2022.9815610.

[22] X. Zhang, J. Li, W. Wu, F. Dong, and S. Wan, "Multi-fault classification and diagnosis of rolling bearing based on improved convolution neural network," *Entropy*, vol. 25, no. 5, p. 737, Apr. 2023, doi: 10.3390/e25050737.

[23] R. Li, S. Li, K. Xu, X. Li, J. Lu, M. Zeng, M. Li, and J. Du, "Adversarial domain adaptation of asymmetric mapping with CORAL alignment for intelligent fault diagnosis," *Meas. Sci. Technol.*, vol. 33, no. 5, May 2022, Art. no. 055101, doi: 10.1088/1361-6501/ac3d47.

[24] Q. Zhang, N. Tang, X. Fu, H. Peng, C. Bo, and C. Wang, "A multi-scale attention mechanism based domain adversarial neural network strategy for bearing fault diagnosis," *Actuators*, vol. 12, no. 5, p. 188, Apr. 2023, doi: 10.3390/act12050188.

[25] F. Ferracuti, A. Freddi, A. Monteriu, and L. Romeo, "Fault diagnosis of rotating machinery based on Wasserstein distance and feature selection," *IEEE Trans. Autom. Sci. Eng.*, vol. 19, no. 3, pp. 1997–2007, Jul. 2022, doi: 10.1109/TASE.2021.3069109.

[26] L. Wan, Y. Li, K. Chen, K. Gong, and C. Li, "A novel deep convolution multi-adversarial domain adaptation model for rolling bearing fault diagnosis," *Measurement*, vol. 191, Mar. 2022, Art. no. 110752, doi: 10.1016/j.measurement.2022.110752.

[27] Y. Zhu, F. Zhuang, J. Wang, G. Ke, J. Chen, J. Bian, H. Xiong, and Q. He, "Deep subdomain adaptation network for image classification," *IEEE Trans. Neural Netw. Learn. Syst.*, vol. 32, no. 4, pp. 1713–1722, Apr. 2021, doi: 10.1109/TNNLS.2020.2988928.

[28] Y. Liu, Y. Wang, T. W. S. Chow, and B. Li, "Deep adversarial subdomain adaptation network for intelligent fault diagnosis," *IEEE Trans. Ind. Informat.*, vol. 18, no. 9, pp. 6038–6046, Sep. 2022, doi: 10.1109/TII.2022.3141783.

[29] Z. Zhang, L. Peng, G. Dai, M. Wang, J. Bai, L. Zhang, and J. Li, "A hybrid adversarial domain adaptation network for bearing fault diagnosis under varying working conditions," *IEEE Trans. Instrum. Meas.*, vol. 72, pp. 1–13, 2023, doi: 10.1109/TIM.2023.3291736.

[30] H. Xiao, L. Dong, W. Wang, and H. Ogai, "Distribution sub-domain adaptation deep transfer learning method for bridge structure damage diagnosis using unlabeled data," *IEEE Sensors J.*, vol. 22, no. 15, pp. 15258–15272, Aug. 2022, doi: 10.1109/JSEN.2022.3186885.

[31] M. Kavianpour, A. Ramezani, and M. T. H. Beheshti, "A class alignment method based on graph convolution neural network for bearing fault diagnosis in presence of missing data and changing working conditions," *Measurement*, vol. 199, Aug. 2022, Art. no. 111536, doi: 10.1016/j.measurement.2022.111536.
[32] Y. Xiao, H. Shao, Z. Min, H. Cao, X. Chen, and J. Lin, "Multi-scale dilated convolutional subdomain adaptation network with attention for unsupervised fault diagnosis of rotating machinery cross operating conditions," *Measurement*, vol. 204, Nov. 2022, Art. no. 112146, doi: 10.1016/j.measurement.2022.112146.
[33] T.-Y. Lin, P. Goyal, R. Girshick, K. He, and P. Dollár, "Focal loss for dense object detection," 2017, *arXiv:1708.02002*.
[34] X. Zhao, J. Yao, W. Deng, M. Jia, and Z. Liu, "Normalized conditional variational auto-encoder with adaptive focal loss for imbalanced fault diagnosis of bearing-rotor system," *Mech. Syst. Signal Process.*, vol. 170, May 2022, Art. no. 108826, doi: 10.1016/j.ymssp.2022.108826.
[35] J. Kuang, G. Xu, T. Tao, and Q. Wu, "Class-imbalance adversarial transfer learning network for cross-domain fault diagnosis with imbalanced data," *IEEE Trans. Instrum. Meas.*, vol. 71, pp. 1–11, 2022, doi: 10.1109/TIM.2021.3136175.
[36] Y. Ganin, E. Ustinova, H. Ajakan, P. Germain, H. Larochelle, F. Laviolette, M. March, and V. Lempitsky, "Domain-adversarial training of neural networks," in *Domain Adaptation in Computer Vision Applications* (Advances in Computer Vision and Pattern Recognition), G. Csurka, Ed. Cham, Switzerland: Springer, 2017, pp. 189–209, doi: 10.1007/978-3-319-58347-1_10.
[37] B. Sun and K. Saenko, "Deep CORAL: Correlation alignment for deep domain adaptation," in *Computer Vision—ECCV* (Lecture Notes in Computer Science), vol. 9915, G. Hua and H. Jégou, Eds. Cham, Switzerland: Springer, 2016, pp. 443–450, doi: 10.1007/978-3-319-49409-8_35.
[38] E. Tzeng, J. Hoffman, N. Zhang, K. Saenko, and T. Darrell, "Deep domain confusion: Maximizing for domain invariance," 2014, *arXiv:1412.3474*.
[39] L. Guo, Y. Lei, S. Xing, T. Yan, and N. Li, "Deep convolutional transfer learning network: A new method for intelligent fault diagnosis of machines with unlabeled data," *IEEE Trans. Ind. Electron.*, vol. 66, no. 9, pp. 7316–7325, Sep. 2019, doi: 10.1109/TIE.2018.2877090.
[40] Q. Wang, G. Michau, and O. Fink, "Domain adaptive transfer learning for fault diagnosis," 2019, *arXiv:1905.06004*.

BO ZHANG received the M.Sc. degree from the School of Measurement and Communication Engineering, Harbin University of Science and Technology, Harbin, China, in 2012. She is currently a Senior Engineer and a Teacher with Guilin University of Aerospace Technology. Her main research interests include intelligent fault diagnosis and domain generalization.

TIANLONG HUO received the M.Sc. degree from Lanzhou University of Technology, in 2011, where he is currently pursuing the Ph.D. degree. He is also a Senior Engineer with Guilin University of Aerospace Technology. His main research interests include fault diagnosis and transfer learning.

ZHENG LIU received the Ph.D. degree from Guilin University of Electronic Technology, Guilin, in 2019. He is currently a Professor with the School of Electronic Engineering and Automation, Guilin University of Aerospace Technology. His research interests include nonlinear systems filtering technology and the control theory of power battery energy management systems.

BAOQUAN HU received the M.Sc. degree from the School of Mechanical and Electrical Engineering, Lanzhou University of Technology, Lanzhou, China, in 2011, where he is currently pursuing the Ph.D. degree with the School of Mechanical and Electrical Engineering. His primary research interests include deep learning and fault diagnosis.

HEYUE HUANG received the M.Sc. degree from Xidian University, Xi'an, China, in 2016. He is currently pursuing the Ph.D. degree with the School of Electronic Engineering and Automation, Guilin University of Electronic Technology, Guilin, China. He is also a Lecturer with the School of Electronic Information and Automation, Guilin University of Aerospace Technology, Guilin. His main research interests include microfluidic, embedded systems, and automatic detection technologies.

ZEHAI REN received the M.Sc. degree from Lanzhou University of Technology, in 2017, where he is currently pursuing the Ph.D. degree. His main research interests include ultraprecision machining and preventive maintenance.

JIANBO JI received the Ph.D. degree in signal and information processing form Shanghai Jiao Tong University, Shanghai, China, in 2016. He has published 17 papers in IEEE journals and conferences. His research interests include communication theory and its applications in practical communication systems, cooperative diversity, and cognitive radio techniques.